

RADAR-BASED “DIURNAL-CYCLE INDICES” FOR HYDROMETEOROLOGY OVER INDONESIAN MARITIME CONTINENT: CONCEPTUAL DISCUSSIONS

M. D. Yamanaka^{*1,2,3}, S. Mori³, H. Hashiguchi⁴, A. Sulaiman⁵, R. Sulistyowati⁵, M. Ogawa⁴, O. Kozan^{1,4}
¹Research Institute for Humanity and Nature (RIHN), ²Kobe University, ³Japan Agency for Marine-Earth Science and Technology (JAMSTEC), ⁴Kyoto University, ⁵Agency of Assessment and Application of Technology (BBPT)

1. INTRODUCTION

Hydrometeorology over Indonesian maritime continent (IMC) is characterized by dominant diurnal cycle rainfalls along the coastlines, for which radar installations, observations and nowcasting have been carried out (Yamanaka et al., 2008, 2016, 2018), because the synoptic analysis and forecasting are almost useless. L-band and VHF wind profilers provide diurnal cycles such as sea-land breeze circulations and raindrop distributions just above stations (Hashiguchi et al., 1995). S-, X- and C-band weather radars show migrations of the diurnal-cycle precipitating cloud systems (Mori et al., 2004, 2018; Wu et al., 2007, 2013).

The diurnal cycle is governed by land-sea (partly mountain-valley) temperature difference with one day periodicity, and its largest cause is the land surface temperature (LST) increase by insolation determined astronomically and dependent on natural or anthropogenic land cover varying geographically. Thus a “standard” diurnal cycle may be analyzed in advance for each area and each season. The sea surface temperature (SST) varied with large-scale interannual variations such as El Niño -southern oscillation (ENSO) and Indian-Ocean dipole mode (IOD), as well as cloudiness affected by intraseasonal variations such as Madden-Julian oscillation (MJO), may be incorporated from global observations. Based on them, we may consider radar-based “diurnal-cycle indices” (DCIs) for predicting rainfall within 24 hours.

2. LOCALLY “STANDARD” DIURNAL CYCLE

Using three-year mean TRMM-PR data, Mori et al. (2004) calculated differences between local AM and PM rainfalls (as in Fig. 1a), which gives a DCI for “standard” diurnal cycle at each location averaged for all phases of intraseasonal, seasonal and interannual variabilities. The AM-PM difference takes positive and negative values on sea and land, respectively. We may calculate it at each location in advance based on accumulated space-borne or ground-based radar observations (e.g., Wu et al., 2003; Araki et al., 2006; Tabata et al., 2011). We may analyze it for each phase of interannual, seasonal or intraseasonal variability (e.g., Kamimera et al., 2012).

As an example, for west Jawa region around Jakarta, diurnal cycle patterns of wind, rainfall and raindrop echo migration are calculated in each day (as in Figs. 1c and g) or for a monthly mean (as in Figs. 1e and i). A pattern in each day is changed probably with an intraseasonal variation, but the peak is almost similar to the monthly-mean value, which is also similar to the longer-period averages such as the original analysis by Mori et al. (2004) for three years.

Other examples for various areas in Sumatera show diurnal-cycle west- and eastward migrations of active convective clouds initiated from the central mountains (Sakurai et al., 2005) (Fig. 2), which are identified with rainfalls observed with the TRMM radar (Mori et al., 2004) and a ground rain gauge (Kozan, 2012) (Fig. 3). An overnight westward migration of diurnal cycle initiated from Kalimantan enhances a local afternoon peak at small islands in the strait and lands on the east coast of Sumatera (As-syakur et al., 2019). Interactions of diurnal cycles are also found between eastern Kalimantan and Sulawesi (Wu et al., 2009) (Fig. 4). For a small island off the west coast of Sumatera, there are two peaks: generated locally in the afternoon, and migrated from Sumatera in the morning (Wu et al., 2008; Kamimera et al., 2012) (Fig. 5). Similar double peaks are observed in a small island near Papua (Tabata et al., 2011) (Fig. 6).

3. DIURNAL-CYCLE “INDICES”

Theoretically a sea-land breeze circulation (SLBC) is driven by the LST-SST difference, and precipitating clouds are developed with ascending motion and moisture transport of SLBC under the conditional instability situation. Since SST varies dominantly with seasonal and interannual scales, the SLBC intensity should be varied mainly with LST. Processes determining LST are studied both observationally and theoretically. The insolation on land during sunrise and noon is responsible for daytime sea wind and evening rainfall on land, and the land rainfall itself is responsible for subsequent midnight land wind and morning rainfall on sea. We may consider several types of DCIs based on radar-based rainfall data at several stations/areas over IMC.

3.1 DCI evaluated from rainfall distribution

A rainfall larger than “standard” diurnal-cycle value in early afternoon suggests an amplification of the diurnal cycle. Therefore, the value of DCI should be adjusted based on real-time radar observations.

* Corresponding author address: Manabu D. Yamanaka, Research Institute for Humanity and Nature, 457-4, Kamigamo-motoyama, Kita-ku, Kyoto 603-8047; e-mail: mdy@chikyu.ac.jp

3.2 DCI based on bright-band inclination

A bright band may be detected in the radar echo around the melting (0°C) level, and its inclination across the coastline corresponds to the land-sea temperature gradient.

3.3 DCI for land rainfall based on sea-side rainfall

Because the diurnal cycle is almost closed in each cycle as considered for the radiative balance in the boundary layer, a morning sea-side rainfall may be correlated with the subsequent evening land-side rainfall, over an appropriate horizontal scale (probably around 10² km).

3.4 Application for floods in cities

Flood disasters are an overriding issue in major cities in the IMC. A diurnal cycle exists also in a river flow (Sulistyowati et al., 2014), and its usual amplitude corresponds to the “standard” diurnal cycle of rainfall analyzed in Section 2. Critical amplitudes causing floods should be related to extreme values of DCIs integrated over a catchment area. A “hazard map” may be built by extreme DCI value distribution.

3.5 Application for dryness in peatlands

Dryness due to less rainfall such as in ENSO and IOD events makes disasters in around peatlands, such as wildfire, smog and health damage. Minimum amplitudes of DCIs and their occurrence tendencies should be studied. Furthermore echoes from the top of a mixing layer containing pollutants and smog may be detected even by a weather radar with suitable specifications (Rahman et al., this conference).

4. CONCLUSION

In this presentation we discuss mainly feasibilities of DCIs for local rainfall in the IMC. However, practical results and usefulness may be realized from examples of radar observations so far made.

References

- Araki, R., and Coauthors, 2006: Seasonal and interannual variations of diurnal cycles of local circulation and cloud activity observed at Serpong, West Jawa, Indonesia. *J. Meteor. Soc. Japan*, **84A**, 171-194. doi:10.2151/jmsj.84A.171
- As-syakur, A. R., and Coauthors, 2019: Analysis of spatial and seasonal differences on diurnal rainfall cycle over Sumatera revealed by 17-year TRMM 3B42 dataset. *SOLA*, submitted.
- Hashiguchi, H., and Coauthors, 1995: Observations of the planetary boundary layer over equatorial Indonesia with an L-band clear-air Doppler radar: initial results. *Radio Sci.*, **30**, 1043-1054. doi: 10.1029/95RS00653
- Kamimera, H., and Coauthors, 2012: Modulation of diurnal rainfall cycle by the Madden-Julian oscillation based on one-year continuous observation with a meteorological radar in west Sumatera. *SOLA*, **8**, 111-114. doi:10.2151/sola.2012-028
- Kozan, O., 2012: Precipitation and groundwater variations in peat swamps. *Studies on Sustainable Humanosphere*, **4**, 271-287. (in Japanese)
- Mori, S., and Coauthors, 2004: Diurnal rainfall peak migrations around Sumatera Island, Indonesian maritime continent observed by TRMM satellite and intensive rawinsonde soundings. *Mon. Wea. Rev.*, **132**, 2021-2039. doi: 10.1175/1520-0493(2004)132:2021:DLRPMO.2.0.CO;2
- Mori, S., and Coauthors, 2018: Meridional march of diurnal rainfall over Jakarta, Indonesia, observed with a C-band Doppler radar: An overview of the HARIMAU-2010 campaign. *Prog. Earth Planet. Sci.*, **5**(47), 1-23. doi:10.1186/s40645-018-0202-9
- Sakurai, N., and Coauthors, 2005: Diurnal cycle of migration of convective cloud systems over Sumatera Island. *J. Meteor. Soc. Japan*, **83**, 835-850. doi:10.2151/jmsj.83.835
- Sulistyowati, R., and Coauthors, 2014: Rainfall-driven diurnal variations of water level in the Ciliwung River, West Jawa, Indonesia. *SOLA*, **10**, 141-144. doi: 10.2151/sola.2014-029
- Tabata, Y., and Coauthors, 2011: Observational study on diurnal precipitation cycle in equatorial Indonesia using 1.3-GHz wind profiling radar network and TRMM precipitation radar. *J. Atmos. Solar Terr. Phys.*, **73**, 1031-1042. doi: 10.1016/j.jastp.2010.10.003
- Wu, P.-M., and Coauthors, 2003: Diurnal variation of precipitable water over a mountainous area in Sumatera Island. *J. Appl. Meteor.*, **42**, 1107-1115. doi: 10.1175/1520-0450(2003)042<1107:DVOPW0>2.0.CO;2
- Wu, P.-M., and Coauthors, 2007: The impact of trans-equatorial monsoon flow on the formation of repeated torrential rains over Java Island. *SOLA*, **3**, 93-96. doi: 10.2151/sola.2007-024
- Wu, P.-M., and Coauthors, 2008: Diurnal variation of rainfall and precipitable water over Siberut Island off the western coast of Sumatera Island. *SOLA*, **4**, 125-128. doi:10.2151/sola.2008-032
- Wu, P.-M., and Coauthors, 2009: The impact of orographically-induced gravity wave on the diurnal cycle of rainfall over southeast Kalimantan Island. *Atmos. Ocean. Sci. Lett.*, **2**, 35-39. doi:10.1080/16742834.2009.11446773
- Wu, P.-M., and Coauthors, 2013: The effects of an active phase of the Madden-Julian oscillation on the extreme precipitation event over western Jawa Island in January 2013. *SOLA*, **9**, 79-83. doi: 10.2151/sola.2013-018
- Yamanaka, M.D., 2016: Physical climatology of Indonesian maritime continent: An outline to comprehend observational studies. *Atmos. Res.*, **178-179**, 231-259. doi: 10.1016/j.atmosres.2016.03.017
- Yamanaka, M.D., and Coauthors, 2008: HARIMAU radar-profiler network over Indonesian maritime continent: A GEOSS early achievement for hydrological cycle and disaster prevention. *J. Dis. Res.*, **3**, 78-88. doi: 10.20965/jdr.2008.p0078
- Yamanaka, M.D., and Coauthors, 2018: Maritime continent coastlines controlling Earth's climate. *Prog. Earth Planet. Sci.*, **5**(21), 1-28. doi:10.1186/s40645-018-0174-9

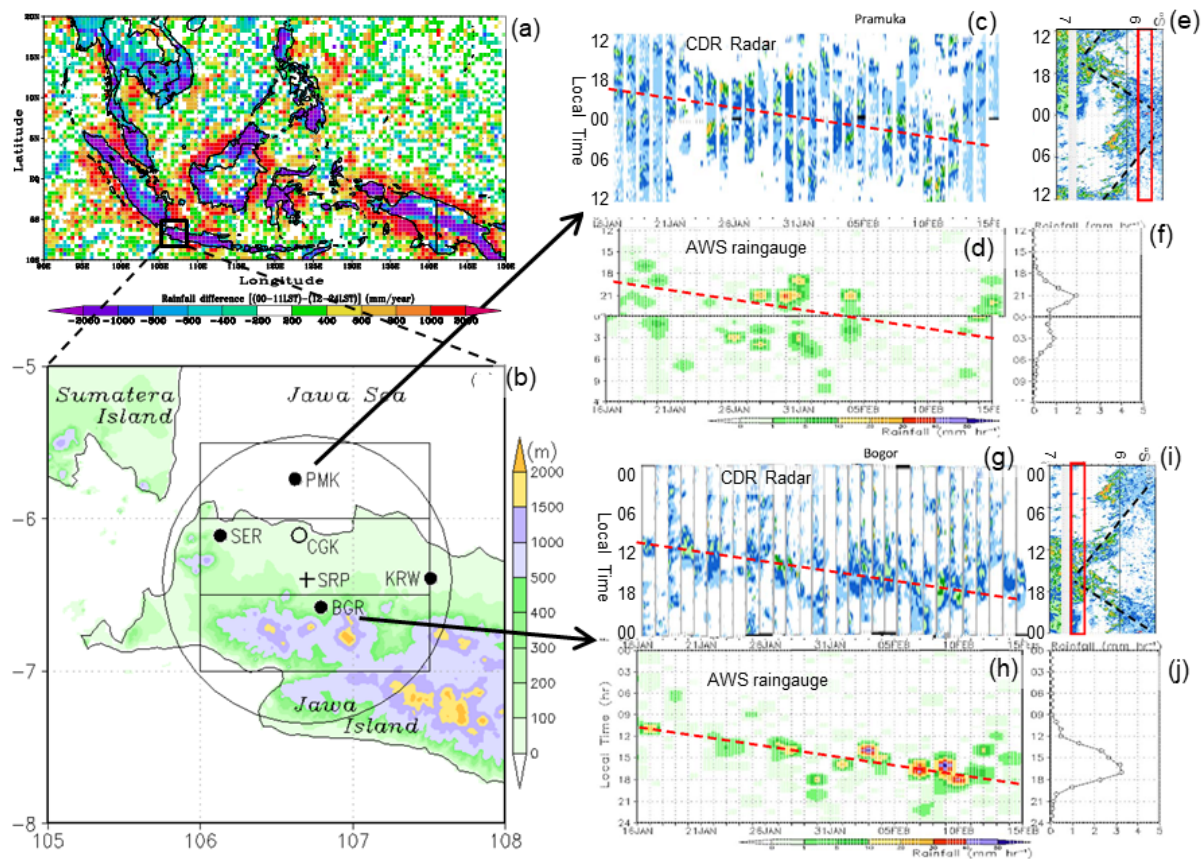


Fig. 1. (a) Distribution of an "original" diurnal cycle index from TRMM in 1998–2000 (Mori et al., 2004, *MWR*). (b) Stations of HARIMAU2010 campaign (16 Jan–15 Feb 2010) with a circle of 105 km range from a C-band Doppler radar (CDR) located at Serpong (SRP) (Mori et al., 2018, *PEPS*). Local time (LT) distributions of (c) CDR and (d) gauge rainfalls at Pramuka Island (PMK) with red dashed lines indicating a delay of 8 h/30days (≈ 16 min/day ≈ 1 cycle/90days). (e) Mean LT-latitude distribution of CDR rainfall with a red rectangle indicating latitudes near PMK. (f) Mean LT distribution of gauge rainfall at PMK. (g)–(j) Same as (c)–(f) but for Bogor (BGR) with LT centered at noon.

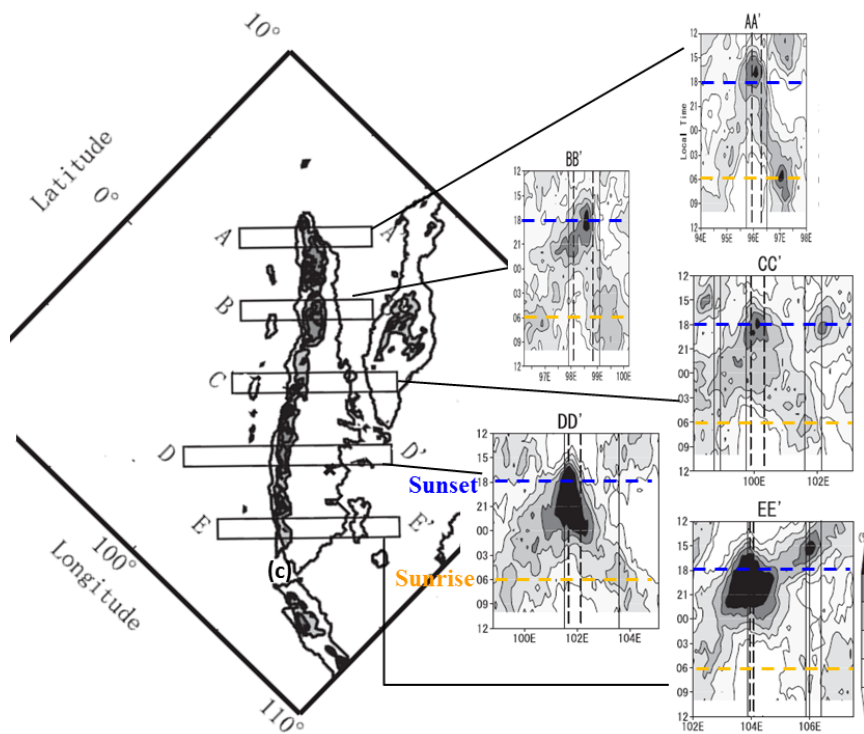


Fig. 2. Geographic variability of diurnal-cycle migrations (Hovmoeller diagrams) of high-GMS cloud top areas, analyzed for five cross-sections approximately perpendicular to the western coastline of Sumatera Island during May 2001–April 2002 (Sakurai et al., 2005).

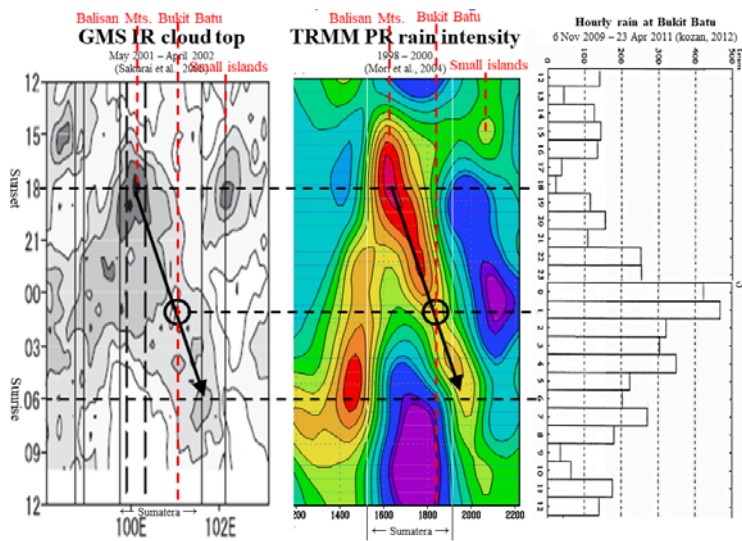


Fig. 3. Comparison between local climatological time-longitude distributions (eastward migrations) of active cloud area (left; Sakurai et al., 2005; Same as CC' in Fig. 2) and rainfall area observed by the TRMM satellite (middle; Mori et al., 2004) and a mean diurnal cycle of rainfall at Bukit Batu village (1°N, 102°E) in the peatland area of Riau (right; Kozan, 2012).

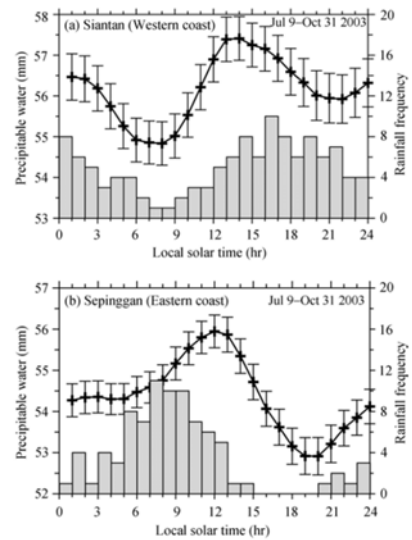


Fig. 4. The mean diurnal variations in GPS-derived precipitable water (line) and rainfall frequency (bar) observed at (a) Siantan on the western coast and (b) Sepinggan on the eastern coast of Kalimantan Island from 9 July to 31 October 2003. The rainfall frequency is the number of hours in which the amount of rainfall exceeded 1.0 mm. The error bars indicate the standard error of the mean. (Wu et al., 2009)

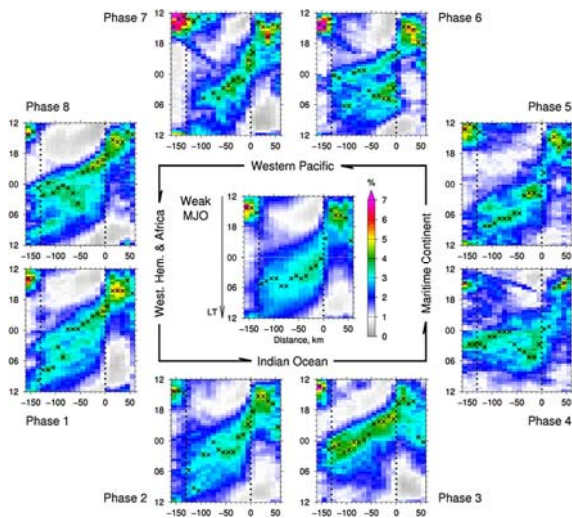


Fig. 5. Distance-time sections of normalized 30-min rainfall for weak MJO condition (central panel) and for each MJO phase. The horizontal axis shows the distance (km) from the west coast of Sumatra (positive toward inland), and the vertical axis shows local time (UTC + 7 h) over one day. Two vertical dotted lines at distances of 0 km and -130 km show the coastlines of Sumatra and Siberut islands, respectively. Cross indicates the peak time of rainfall DC at each distance. (Kamimera et al., 2012)

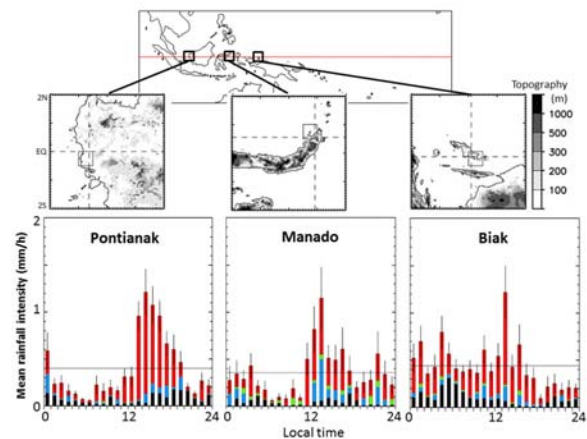


Fig. 6. Diurnal cycles of rainfall intensity observed by wind profilers at Pontianak (Kalimantan), Manado (Sulawesi) and Biak (near Papua) (Tabata et al., 2011). Rainfall is classified as stratiform (black), mixed stratiform/convective (blue), shallow convective (green) and deep convective (red) types. In particular, a small island like Biak has double peaks: one is generated locally in the afternoon, and the other (appearing before dawn in this case) migrates from a neighboring large island.